Technology

Analytical Study for Mechanism of Localized Corrosion Developed by Microscopic Electrochemical Measurement

Hiroyuki FUJI*

Abstract

Localized corrosion in steel initiates in a narrow area at the microscale level. Therefore, it is difficult to analyze the initiation site of localized corrosion by the conventional electrochemical measurement whose electrode area is about 1 cm^2. To clarify the mechanism of localized corrosion, microscopic electrochemical measurement whose electrode area is about 0.01 mm^2 is effective, because the measurement evaluates the electrochemical characteristics of specific inclusions where the localized corrosion initiates. This paper focused on the pitting initiates at the MnS inclusions in the surface of low-alloy steel at a pH of 8.0. The applications of microscopic electrochemical measurement such as the measurements combined with the electrochemical test under tensile stress, and with in-situ Raman spectroscopy are presented with data.

1. Introduction

According to a study conducted in 2015, the total expenditure on corrosion control measures in Japan reached 6.5 trillion yen, equivalent to 1.25% of the gross national income (GNI).[1] **Figure 1** illustrates the trend in costs associated with corrosion control measures, specifically within the energy sector (including water, electricity, and gas). In fiscal 2015, the cost of corrosion control measures in this sector amounted to 802.2 billion yen, marking a significant increase of 13.5 times compared to fiscal 1974.[1] Among these expenses, maintenance costs constitute the majority, accounting for approximately 88% of the overall expenditure.[1] This highlights the growing significance of equipment maintenance and preservation efforts. To address this escalating cost burden related to corrosion control measures, one approach from a material perspective is to develop materials with exceptional corrosion resistance capabilities, promote maintenance-free construction methods, and propose fitting materials and solutions tailored for specific operating environments with varying severity levels. Achieving these goals necessitates a comprehensive understanding of corrosion mechanisms.

Sulfide stress cracking (SSC) and stress corrosion cracking (SCC) pose significant challenges for energy tubular products. These cracks are known to initiate localized corrosion called pitting, with stress concentration occurring at the bottom of pits and leading to crack propagation.[2] Enhancing the pitting corrosion resistance of

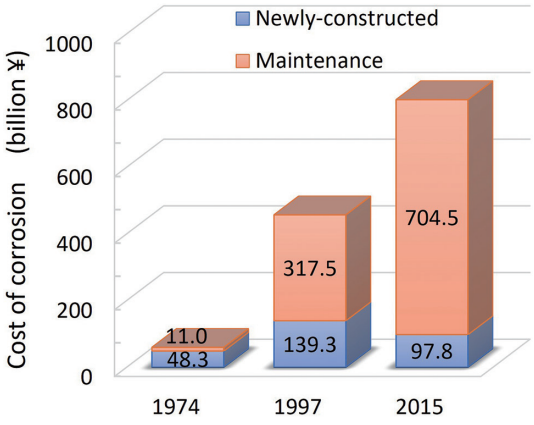

Fig. 1 Transient cost of corrosion in energy field

energy tubular products has proven effective in improving resistance against SSC and SCC. However, the mechanisms and factors influencing pitting corrosion still need to be better understood. This study presents our established method for microscopic electrochemical measurements aimed at elucidating the pitting corrosion mechanism in low-alloy steels as a precursor process to SSC and SCC. Additionally, we report the application technologies associated with

* Researcher, Steel Products Research Dept., Kansai R & D Lab.
1-8 Fuso-cho, Amagasaki City, Hyogo Pref. 660-0891

this microscopic electrochemical measurement method.

2. Microscopic Electrochemical Measurement Method and its Applications

2.1 Microscopic electrochemical measurement method

Pitting corrosion is a localized form of corrosion that occurs in microscopic regions, typically originating from inclusions several micrometers in diameter. Conventional electrochemical measurements performed on test areas of approximately 1 cm^2 cannot accurately analyze the process by which pitting corrosion develops. To overcome this limitation, microscopic electrochemical measurement methods have been developed to assess the electrochemical properties of specific inclusions responsible for corrosion by focusing on microscopically small regions on the order of micrometers.[3–6] Microscopic electrochemical measurements can be broadly categorized into masking and capillary cell methods (**Fig. 2**). The masking method involves coating the entire specimen with resin, except for the area containing the targeted inclusions, and then testing the specimen. Conversely, the capillary cell method entails placing the tip of a tube called a capillary cell near the inclusion being measured and conducting electrochemical measurements inside this confined space. In our research, we have utilized microscopic electrochemical measurements employing the masking method. Furthermore, we have developed test apparatuses for applying tensile stress to the specimen during electrochemical tests and techniques for combining in-situ analysis using Raman spectroscopy. Currently, we are conducting an extensive analysis to elucidate the detailed mechanisms underlying the occurrence of pitting corrosion.

2.2 Analysis of effect of stress on occurrence of pitting corrosion

Stress is a significant contributing factor to the occurrence of SSC and SCC. In the case of tubular products used in energy extraction, the energy tubular product structures experience tensile stress due to factors such as internal pressure from production fluids, their weight, and formation pressure.[2] To investigate the impact of tensile stress on pitting corrosion, we developed a test cell capable of conducting electrochemical measurements under stress conditions. **Figure 3** presents a schematic diagram illustrating the electrochemical test cell. To apply stress to the specimen, the specimen was positioned vertically. So, the test cell was designed to be horizontally attached to the specimen. We utilized a sustained-load device (commonly referred to as a proof ring) for stress loading. The testing machine is typically used to assess the susceptibility to cracking in round bar test specimens by subjecting them to a corrosive environment while applying tensile stress to them. We modified the testing machine by improving its specimen grips specifically for applying tensile stress to the plate test specimen.[7] A 0.24 mass%C-0.97 mass%Mn-0.011 mass%S-Fe steel with the Mn and S contents increased enough to form manganese sulfide (MnS) inclusions within the steel matrix was melted in a laboratory and tested. **Figure 4** displays the polarization curves (current-potential curves) obtained using microelectrodes with a test area measuring approximately 0.01 mm^2 in a 0.02 $molL^{-1}$ NaCl containing borate buffer solution (pH 8.0) after deaeration with N_2 gas. In this study, potential values are expressed relative to an Ag/AgCl electrode (saturated KCl) and denoted as V vs SSE. The higher current density on the vertical axis indicates higher corrosion rates observed during testing. The applied stress was 90% of the 0.2% proof stress (426 MPa) (hereafter referred to as 90%AYS). In the absence of stress, a corrosion potential appeared at about −0.55 V. As the potential increased, a current peak due to an active dissolution emerged. Subsequently, an oxide film formed on the steel surface, leading to passivation and a decrease in current density. A further potential increase resulted in a sudden current surge around 0 V, indicative of pitting corrosion. When 90%AYS was applied to the specimen, the current density passed through an active state peak. It did not decline to a passive state but

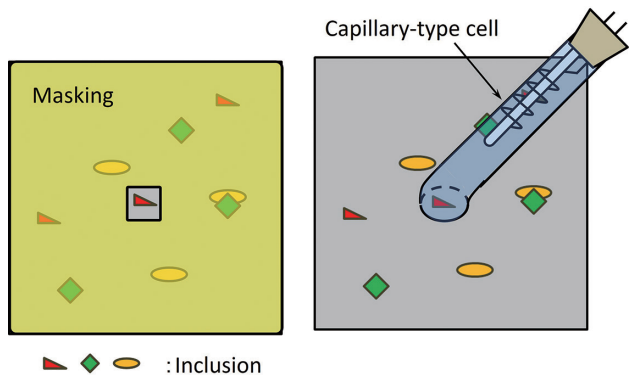

Fig. 2 Schematic of microscopic electrochemical test
Left: Masking method, Right: Capillary-cell method

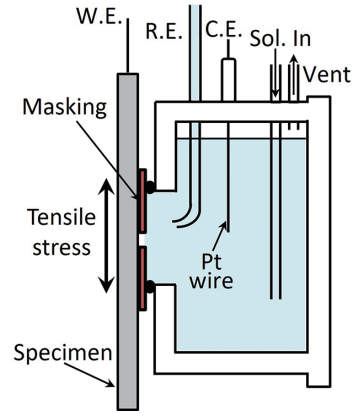

Fig. 3 Schematic of the electrochemical test cell under tensile stress

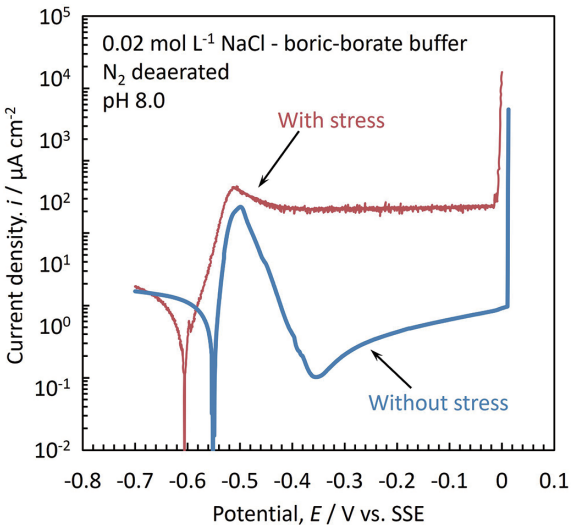

Fig. 4 Microscopic polarization curves with and without stress (Test area: approx. 0.01 mm^2)

leveled off in the active dissolution current region. Optical microscope images before and after the test are shown in **Fig. 5**. It is revealed that pitting corrosion is consistently initiated from MnS under all test conditions, regardless of stress presence. SEM observation focused on the dissolution behavior near MnS. Unfortunately, in the 90%AYS-loaded specimen, the MnS responsible for pitting corrosion detached during washing and could not be confirmed by SEM. **Figure 6** displays the SEM results of MnS after the test. Without stress, pitting occurred at the interface between MnS and the base metal. No dissolution was observed in MnS itself or at the interface, except in regions where pitting occurred. Under 90%AYS, the MnS and base metal interface melted, forming a crevice. MnS itself also dissolved as shown in Fig. 6.

The above findings indicate that stress enhances the dissolution of MnS as well as the interface between MnS and the base metal, leading to introduction of the initiation site of pitting. This stress-induced dissolution hinders the formation of a passive film, resulting in decreased resistance to pitting corrosion.

2.3 In-situ analysis of dissolution products of inclusions

In this section, we report the results of in-situ Raman spectroscopy analysis of MnS while performing microscopic electrochemical measurements in order to identify the chemical species generated as with the dissolution of MnS. **Figure 7** shows a schematic diagram of the test cell. An electrochemical cell for optical observation with a quartz window was used as the test cell. Electrochemical measurements were performed under the same conditions as described in the previous section, using the microscopic region containing MnS shown in **Figure 8** as the test surface. This test was conducted under stress-free conditions. During the test, Raman spectroscopy on MnS was performed while observing the test surface in situ. **Figure 9** shows a polarization curve measured using an electrochemical cell for optical observation. Like the polarization curves shown in Fig. 4, the polarization curve in Fig. 9 showed a current peak attributed to an active dissolution, a passive state re-

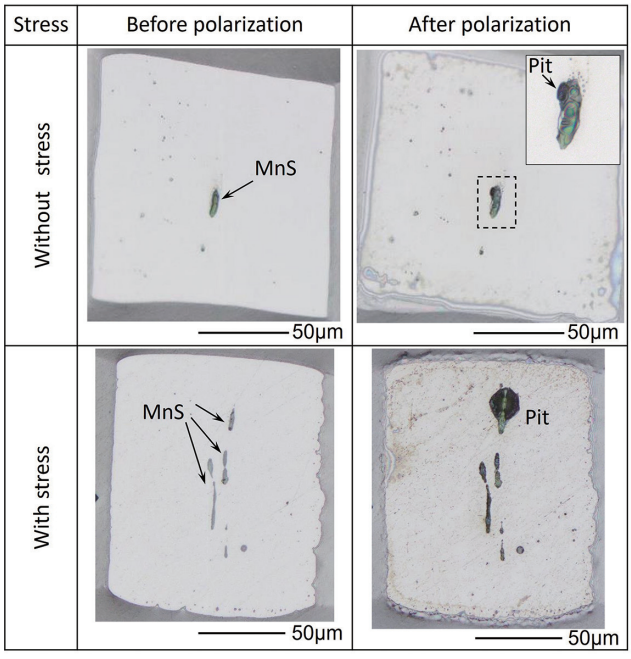

Fig. 5 Optical micrographs of masked areas before and after polarization
Upper row: Without stress, Lower row: With stress

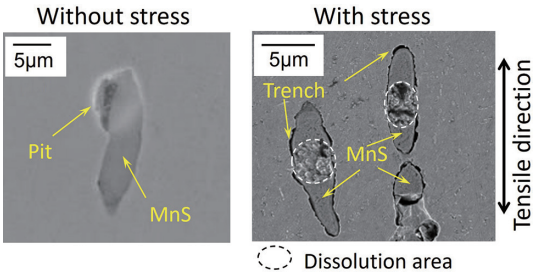

Fig. 6 SEM images of MnS inclusions after polarization with and without stress

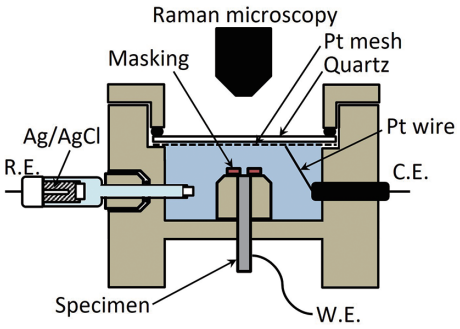

Fig. 7 Schematic of the electrochemical test cell with Raman spectroscopy

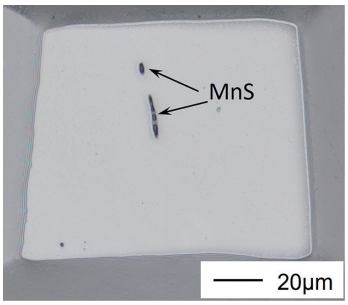

Fig. 8 Optical micrograph of masked area including MnS

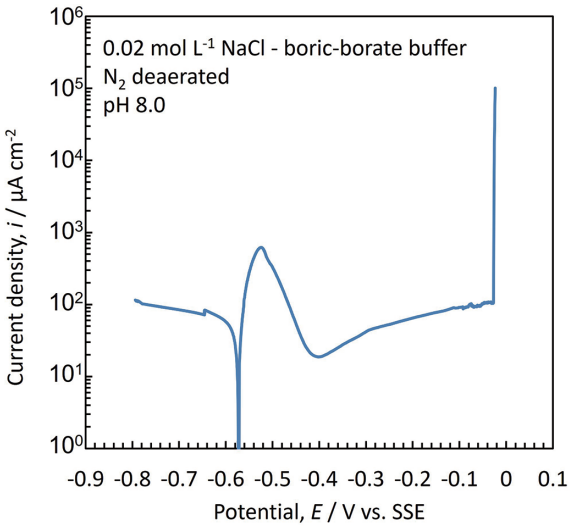

Fig. 9 Microscopic polarization curve using electrochemical test cell with optical observation

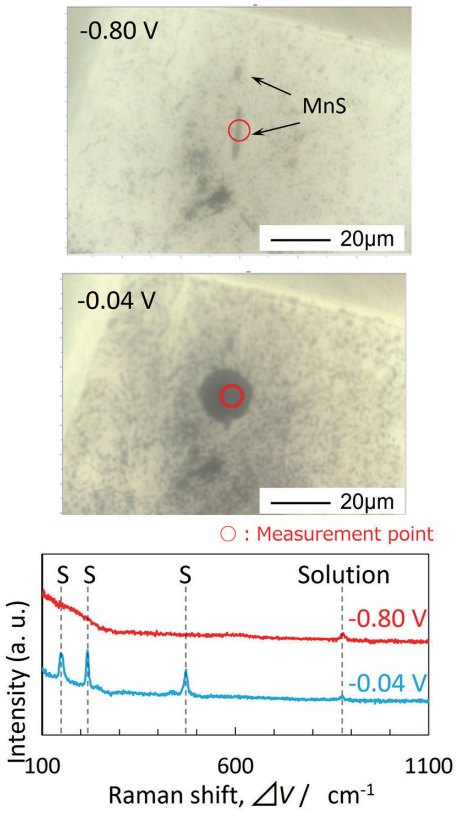

Fig. 10 Optical micrographs of MnS inclusions, and microscopic Raman spectra on MnS at −0.80 and −0.04 V

gion, and a rapid current increase associated with the occurrence of pitting corrosion. **Figure 10** shows in-situ optical micrographs and Raman spectra of the specimen surface. Pitting corrosion originated from the MnS inclusion with a length of about 20 μm, which was the lower one of the two MnS inclusions on the specimen surface. The electrode potential at this time was −0.04 V. Comparison of the Raman spectra revealed that only one peak due to the test solution was detected at the electrode potential of −0.80 V, where the polarization started. On the other hand, at the electrode potential of −0.04V, where pitting corrosion occurred, a new peak due to S atoms (elemental sulfur) was detected in addition to the peak due to the test solution. Therefore, this analysis revealed that when pitting corrosion originates from MnS in low-alloy steel, S atoms are generated as the dissolution products of MnS. Regarding the influence of S atoms on corrosion, a mechanism has been reported in which S atoms adsorbed on the stainless steel surface promote the dissolution of the interface between MnS and the base metal and promote pitting corrosion[8] as well as another mechanism in which the reduction reaction rate on the surface of Ni-based alloy is accelerated to increase the SCC susceptibility.[9] Understanding how S atoms affect pitting corrosion and crack propagation within low-alloy steel remains an important area for future research.

3. Conclusion

This study aimed to investigate the mechanism of pitting corrosion as a precursor to sulfide stress cracking (SSC) and stress corrosion cracking (SCC) in tubular products used for energy extraction and production. We have developed the applications of microscopic electrochemical measurements to analyze pitting behavior in low-alloy steel as described above. To fully understand the mechanism of localized corrosion, it is crucial to comprehensively study phenomena at both micro and macro scales, including corrosion occurrence and crack growth. Our goal is to advance our understanding of corrosion mechanisms by incorporating the latest analysis technologies that are continuously evolving.

Acknowledgments

The corrosion analysis technique presented in this paper was established through joint research with Tohoku University (Multiscale Materials (Nippon Steel) Joint Research Division). We would like to express our sincere gratitude to Professor Izumi Muto, Visiting Professor Takuya Hara, and Assistant Professor Masashi Nishimoto of Tohoku University for their valuable guidance and support.

References

1) Japan Society of Corrosion Engineering, Japan Association of Corrosion Control: Cost of Corrosion in Japan (electronic version of survey report), 2020, 284p
2) Omura, T. et al.: Nippon Steel & Sumitomo Metal Technical Report. (107), 19 (2015)
3) Böhni, H. et al.: Electrochim. Acta. 40 (10), 1361 (1995)
4) Fushimi, K. et al.: ISIJ Int. 56 (3), 431 (2016)
5) Muto, I. et al.: Zairyo-to-Kankyo. 67 (5), 197 (2018)
6) Kadowaki, M. et al.: Zairyo-to-Kankyo. 67 (12), 497 (2018)
7) Trillo, E. et al.: CORROSION/2019, Paper No. 12908, NACE International, Houston, 2019
8) Chiba, A. et al.: J. Electrochem. Soc. 160 (10), C511 (2013)
9) Miyasaka, A. et al.: Corrosion. 45 (9), 771 (1989)

Hiroyuki FUJI
Researcher
Steel Products Research Dept.
Kansai R & D Lab.
1-8 Fuso-cho, Amagasaki City, Hyogo Pref. 660-0891